American Journal of Environmental Science and Engineering
2026, Vol. 10, No. 4, pp. 164–171
https://doi.org/10.11648/j.ajese.20261004.16

Research Article

Alkali Metal Potassium-Synergistically Driven Dual-Phase High-Entropy Layered Double Hydroxide/Spinel Heterostructure for Efficient Oxygen Evolution Reaction

Xin Li, Bin Dong*, Yong-Ming Chai

College of Chemistry and Chemical Engineering, China University of Petroleum (East China), Qingdao, China

Abstract

The sluggish kinetics of the anodic oxygen evolution reaction (OER) in water electrolysis for hydrogen production and its heavy dependence on noble metal catalysts restrict the large-scale application of green hydrogen energy. In this work, we designed and prepared a self-supported dual-phase high-entropy layered double hydroxide/spinel (HELDH/HESO) heterostructured oxygen evolution electrocatalyst, (K)-NiCoFeCrCe-HELDH/HESO@NF, synergistically driven by alkali metal potassium (K). Through a one-step hydrothermal method, six metal salts containing K, Ni, Co, Fe, Cr, and Ce were co-deposited on a nickel foam (NF) substrate, yielding a self-supported electrode with a three-dimensional nanosheet structure and moderate pore size. The introduction of catalytically inactive alkali metal K into the lattice induces lattice expansion and distortion, optimizes the electronic density of states of adjacent transition metals (Ni, Co, Fe), and regulates the d-band center position, thereby optimizing the adsorption free energies of oxygen-containing intermediates (OH*, O*, OOH*) and significantly enhancing the intrinsic OER activity. The dual-phase LDH/spinel heterointerfaces provide high-density defects and unsaturated coordination sites, strengthening interfacial electronic regulation. In 1 M KOH electrolyte, (K)-NiCoFeCrCe-HELDH/HESO@NF requires only overpotentials of 279 mV and 355 mV to achieve current densities of 100 mA cm^{-2} and 1000 mA cm^{-2}, respectively, outperforming the K-free counterpart electrode. In an anion exchange membrane (AEM) electrolyzer under simulated industrial conditions, the electrode operated continuously at a constant current of 1 A for 100 h with only about 6.4% voltage increase, demonstrating excellent long-term stability. The preparation process is simple, reproducible, cost-controllable, and environmentally friendly, offering a new strategy for the development of efficient, stable, and low-cost non-noble-metal OER catalysts.

Keywords

Oxygen Evolution Reaction, High-entropy Materials, Heterostructures, Water Electrolysis for Hydrogen Production, Anion Exchange Membrane Electrolyzer

*Correspondence:Bin Dong (dongbin@upc.edu.cn)

Received: 9 October 2026; **Accepted:** 3 November 2026; **Published:** 10 November 2026

Copyright: © The Author(s), 2026. Published by Science Publishing Group. This is an **Open Access** article, distributed under the terms of the Creative Commons Attribution 4.0 License (http://creativecommons.org/licenses/by/4.0/), which permits unrestricted use, distribution and reproduction in any medium, provided the original work is properly cited.

1. Introduction

Fossil fuels are finite, and their continued use is running into resource depletion, environmental pollution, and carbon emissions. To move toward a low-carbon energy system and green, sustainable development, China has set clear "dual carbon" goals: peaking carbon emissions before 2030 and reaching carbon neutrality by 2060 [1-3]. This has spurred rapid growth in renewable power generation, including solar, wind, and hydropower. However, these sources are inherently intermittent and variable, which makes large-scale, high-penetration grid integration difficult, and surplus electricity is hard to store and use efficiently. Hydrogen—a clean and efficient secondary energy carrier—offers a promising way to convert and store surplus renewable electricity. Water electrolysis for hydrogen production has therefore become a key route to large-scale green hydrogen production [4].

At present, hydrogen production via water electrolysis mainly follows four technological routes: alkaline water electrolysis (ALK), proton exchange membrane water electrolysis (PEM), high-temperature solid oxide electrolysis (SOEC), and anion exchange membrane water electrolysis (AEM) [5-7]. AEM water electrolysis combines the low cost of ALK with the simplicity and high efficiency of PEM. It features high hydrogen purity, fast system response, and good gas tightness, making it well matched to the intermittent and fluctuating output of renewable power generation, while also allowing a broad choice of catalysts for the membrane electrode assembly. However, AEM water electrolysis involves two half-reactions: the anodic oxygen evolution reaction (OER) and the cathodic hydrogen evolution reaction (HER). OER is a complex four-electron transfer process with sluggish kinetics and a relatively high overpotential, which restricts the overall energy conversion efficiency and economic feasibility [8, 9]. At the same time, high-performance catalysts still rely on noble metals such as Ir and Ru, keeping costs high. Therefore, developing efficient, highly stable, and low-cost non-noble-metal OER electrocatalysts has become key to advancing the large-scale deployment of this technology [10].

Over the past few years, high-entropy materials (HEMs) have shown considerable promise in electrocatalytic OER, largely because of their unique multi-element synergy and tailorable electronic structures [11]. Typically, such materials are composed of five or more metals in equal or nearly equal molar ratios, leading to a highly disordered atomic arrangement along with plentiful surface defects and active sites . This high-entropy design strategy has further been expanded to layered double hydroxides (LDHs), producing high-entropy LDHs that offer greater elemental variety and structural adjustability [12]. However, the multi-component nature of HEMs makes it challenging to achieve an ideal trade-off between catalytic activity and structural durability. Moreover, the entropy-induced complexity of inter-component interactions can adversely affect electron transport and reaction kinetics [13, 14]. Thus, how to realize effective cooperation among metal components and concurrently optimize both activity and stability is a key scientific issue for advancing HEMs in OER [15].

Heterostructure engineering has proven to be an effective route to improved OER performance [16]. Heterointerfaces tend to create abundant defect sites and dangling bonds, which can act as additional catalytic centers with high intrinsic activity. Owing to the work-function difference between the two phases, directional electron transfer and redistribution occur at the interface, thereby optimizing the adsorption free energies of oxygen-containing intermediates (OH*, O*, OOH*) on the active sites and effectively lowering the reaction overpotential and the energy barrier of the rate-determining step [17, 18]. Yet heterostructures also face issues such as poor interfacial stability, uncertain resistance, and ambiguous active sites. The high-entropy heterostructure design concept achieves directional control over the electronic structure by constructing multi-metal active sites. Its entropy stabilization effect and sluggish ion-migration kinetics help suppress phase evolution and metal-ion dissolution during electrochemical processes, pointing the way toward efficient and stable non-noble-metal OER catalytic systems [19-21].

Alkali metal ions, with their low electronegativity and large ionic radius, can be introduced into oxide/hydroxide lattices as non-catalytically active species. Their incorporation causes lattice expansion and distortion, which helps tune the electronic density of states of nearby transition metals and shift the d-band center. This, in turn, optimizes the adsorption free energies of oxygen-containing intermediates and boosts intrinsic OER activity [22-25]. Building on this idea, we designed and prepared a self-supported dual-phase high-entropy layered double hydroxide/spinel (HELDH/HESO) heterostructured electrode, (K)-NiCoFeCrCe-HELDH/HESO@NF, in which alkali metal potassium (K) acts as a synergistic driver. A one-step hydrothermal method was used to co-deposit six metal salts—K, Ni, Co, Fe, Cr, and Ce—on nickel foam. The resulting electrode takes advantage of high-entropy effects, heterointerface synergy, and K-mediated electronic regulation simultaneously. Its structure and electrocatalytic OER performance were systematically studied, and its potential for industrial use was further confirmed in an anion exchange membrane electrolyzer.

2. Materials and Methods

Nickel foam (NF; 1 cm × 8 cm) was ultrasonically cleaned in 1 M HCl, acetone, and anhydrous ethanol for 20–30 min in sequence. After rinsing with deionized (DI) water, it was dried in a vacuum oven at 60 °C and set aside for use. $Ni(NO_3)_2·6H_2O$, $Co(NO_3)_2·6H_2O$, $Fe(NO_3)_3·9H_2O$, $Cr(NO_3)_3·9H_2O$, and $Ce(NO_3)_3·6H_2O$ were dissolved in 35 mL DI water. The total transition-metal amount was fixed at 2 mmol, with the Ni:Co:Fe:Cr:Ce molar ratio at

0.4:0.4:0.4:0.4:0.4 (0.4 mmol each). KNO_3 was then added to give K:(Ni+Co+Fe+Cr+Ce) = 0.8:2. The mixture was magnetically stirred for 5 min until homogeneous. Urea (12 mmol) and NH_4F (8 mmol) were added, and stirring continued for another 5 min. The resulting solution was transferred together with the pretreated NF into an 80 mL PTFE liner, sealed in a stainless-steel autoclave, and heated at 120 °C for 8 h. This produced an NF-supported dual-phase high-entropy layered double hydroxide/spinel heterostructured electrode, denoted (K)-NiCoFeCrCe-HELDH/HESO@NF. The obtained sample was washed alternately with DI water and 95% ethanol until the washings became neutral, then vacuum-dried at 60 °C. To assess the role of potassium, a K-free control electrode, NiCoFeCrCe-HELDH/HESO@NF, was prepared under identical conditions except that KNO_3 was omitted.

The sample morphology was analyzed using a Zeiss Sigma 500 scanning electron microscope (SEM), and the elemental composition and distribution were determined by an Oxford X-Max energy-dispersive spectrometer (EDS). The crystal structure was analyzed with a Haoyuan DX-2700BH X-ray diffractometer (XRD, Cu Kα radiation, 40 kV, 30 mA, scanning range 2θ = 10°-80°, scan rate 5°/min).

The oxygen evolution performance was evaluated using a Gamry Reference 3000 electrochemical workstation (USA). A three-electrode system was employed: Hg/HgO as the reference electrode, platinum foil as the counter electrode, and the prepared electrode as the working electrode, with 1 M KOH aqueous solution as the electrolyte. The potential was converted to reversible hydrogen electrode (RHE) scale using the equation E(RHE) = E(Hg/HgO) + 0.059 × pH + 0.098. Long-term stability tests were conducted in an anion exchange membrane (AEM) electrolyzer using chronoamperometry at a constant current of 1 A for continuous operation over 100 hours.

3. Results and Discussion

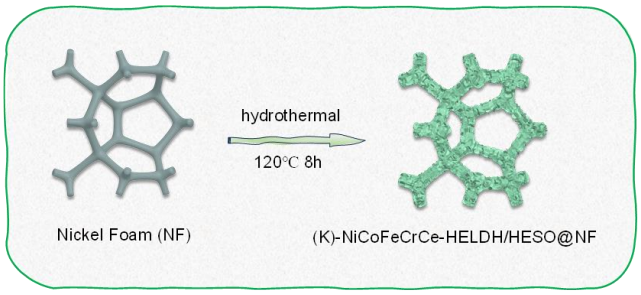


Figure 1. *Schematic diagram of the synthesis of the (K)-NiCoFeCrCe-HELDH/HESO@NF.*

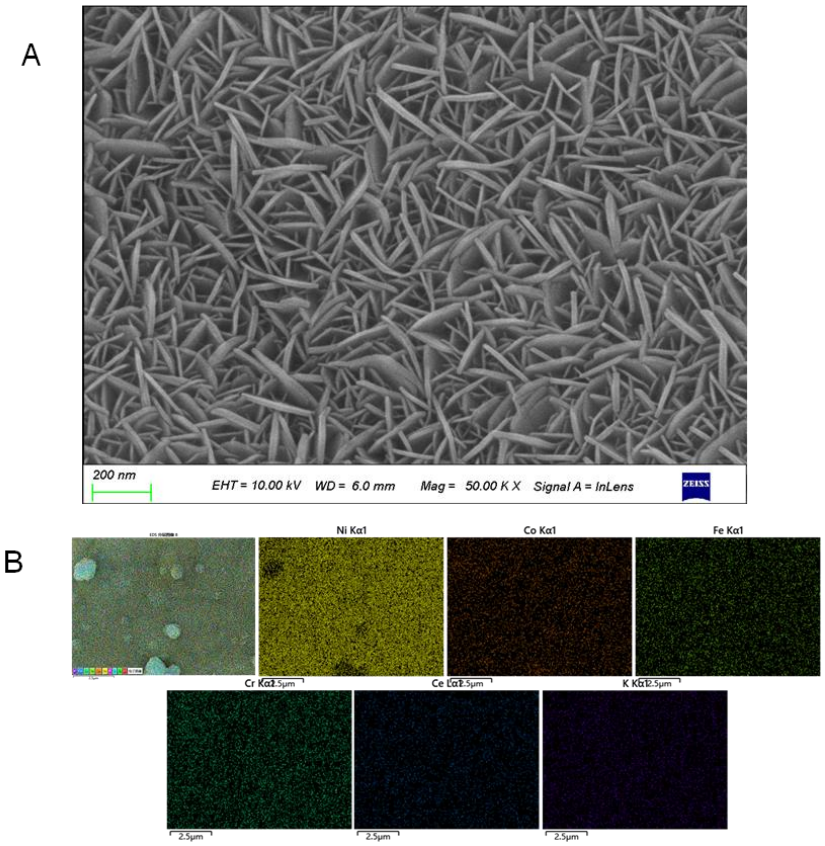


Figure 2. *(A) SEM images of (K)-NiCoFeCrCe-HELDH/HESO@NF. (B) Elemental distribution maps of (K)-NiCoFeCrCe-HELDH/HESO@NF.*

Figure 1 illustrates the preparation route of (K)-NiCoFeCrCe-HELDH/HESO@NF. The high-entropy (K)-NiCoFeCrCe-HELDH/HESO@NF was grown in situ on NF via hydrothermal synthesis. Figure 2A presents SEM images, revealing that the surface of the (K)-NiCoFeCrCe-HELDH/HESO@NF electrode exhibits a three-dimensional nanosheet architecture, with individual nanosheets approximately 200–600 nm in lateral size. This two-dimensional nanosheet structure endows the material with a relatively large specific surface area, which helps expose more catalytically active sites and facilitates rapid electron transport and transfer. The suitable pore channels on the surface also promote the transport and adsorption/desorption of the alkaline electrolyte and reaction intermediates. Figure 2B shows EDS analysis results: the six elements K, Ni, Co, Fe, Cr, and Ce are uniformly distributed across the electrode surface, confirming that the high-entropy multi-metal components underwent homogeneous co-precipitation during hydrothermal co-deposition, with elemental segregation effectively suppressed.

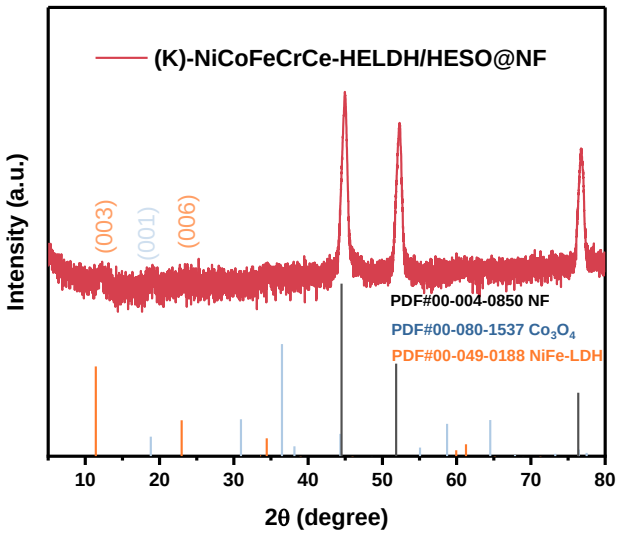


Figure 3. *XRD images of (K)-NiCoFeCrC-HELDH/HESO@NF.*

Figure 3 presents the XRD pattern. Peaks appear at roughly 11.6°, 23.4°, 34.5°, and 39.1°. Based on the standard database (PDF#049-0188), these correspond to the (003), (006), (012), and (015) reflections of a hexagonal NiFe-LDH structure. A peak near 18.9° matches the Co3O4 spinel phase (PDF#080-1537). Together, these results show that the sample contains both a high-entropy layered double hydroxide phase and a spinel phase, i.e., a dual-phase heterostructure. The interface region between the two phases usually has a high density of defects and unsaturated coordination sites, which can act as efficient catalytic active centers. The two phases are also tightly bound, which helps prevent elemental segregation and preserve structural stability.

To evaluate the OER performance of (K)-NiCoFeCrCe-HELDH/HESO@NF, electrochemical measurements were carried out in 1 M KOH using the standard three-electrode configuration shown in Figure 4. OER activity of (K)-NiCoFeCrCe-HELDH/HESO@NF and the K-free control electrode was then compared by linear sweep voltammetry (LSV). At a current density of 100 mA cm^{-2}, the overpotential of the K-containing electrode was 279 mV, whereas the K-free electrode required 299 mV. When the current density was increased to 1000 mA cm^{-2}, the corresponding overpotentials were 355 mV and 389 mV, respectively. Thus, the K-containing electrode lowered the overpotential by 20 mV at 100 mA cm^{-2} and by 34 mV at 1000 mA cm^{-2}. The larger overpotential gap at high current density indicates that K doping not only improves the intrinsic activity of the material but also helps maintain favorable reaction kinetics under more demanding operating conditions. This performance enhancement can be explained by the combined electronic and structural effects introduced by K. Because K has low electronegativity and a large ionic radius, its incorporation into the HELDH lattice causes lattice expansion and distortion. This perturbation alters the electronic density of states of neighboring Ni, Co, and Fe and shifts the d-band center, thereby optimizing the adsorption free energies of the oxygen-containing intermediates OH*, OOH*, and O* and lowering the energy barrier of the rate-determining step. As a result, the intrinsic OER activity is enhanced. Since both the K-doped electrode and the K-free electrode share the same high-entropy LDH/spinel framework, the lower overpotential of the (K)-electrode specifically highlights the electronic modulation role of K, rather than merely compositional or morphological differences. The dual-phase heterointerface and high-entropy matrix further reinforce this effect. The LDH/spinel interface provides abundant defects and unsaturated coordination sites that can serve as additional active centers; meanwhile, the work-function difference between the two phases drives directional electron transfer and redistribution at the interface, thereby tuning intermediate binding and interfacial charge transport. The high-entropy composition contributes to entropy stabilization and sluggish ion-migration kinetics, thus suppressing metal-ion leaching and phase transformation during electrocatalysis. In addition, the three-dimensional nanosheet structure and suitable pore channels facilitate electrolyte penetration, intermediate diffusion, and gas bubble release. Collectively, these features explain why (K)-NiCoFeCrCe-HELDH/HESO@NF exhibits significantly lower overpotentials than the K-free control at both moderate and high current densities.

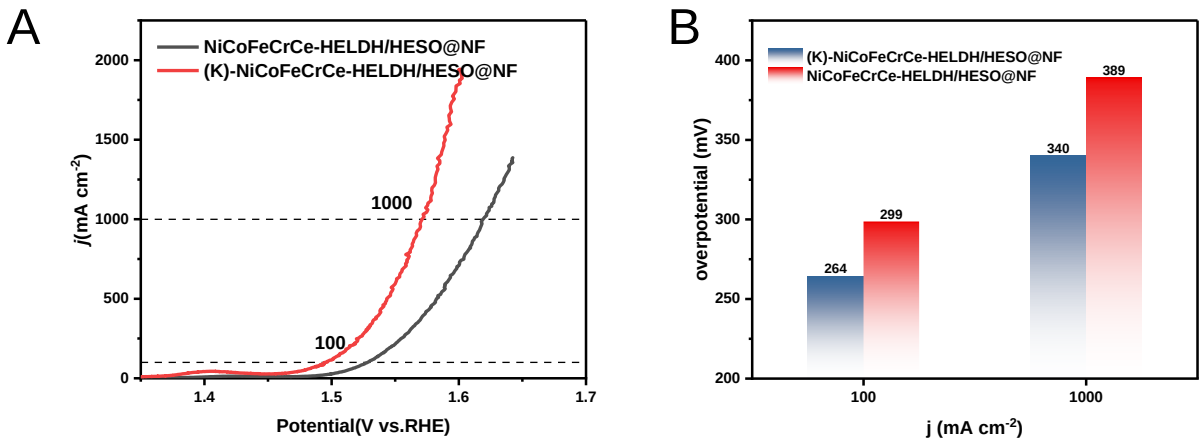


Figure 4. *A) LSV curves of (K)-NiCoFeCrCe-HELDH/HESO@NF. (B) Overpotentials in η100 and η1000.*

To assess how (K)-NiCoFeCrCe-HELDH/HESO@NF performs under practical conditions, we carried out a long-duration stability test in an anion exchange membrane water electrolyzer (AEMWE), aiming to gauge its feasibility for industrial-scale hydrogen production. Figure 5A depicts the assembled AEMWE setup, and Figure 5B provides the corresponding stability profile. At room temperature and an industrially relevant current density of 1 A cm^{-2}, the cell voltage rose only from 2.18 to 2.32 V after more than 100 h of continuous operation—an increase of roughly 6.4%. This indicates outstanding durability and meets the long-term operation demands of an AEM water electrolysis system under simulated industrial conditions. The stable behavior can be traced to several coupled mechanisms. Potassium incorporation into the HELDH lattice causes lattice expansion and distortion, altering the electronic density of states of adjacent Ni, Co, and Fe and displacing the d-band center. Accordingly, the adsorption free energies of OH, *O*, and OOH* become more favorable. Meanwhile, the barrier associated with the rate-determining step is reduced. Which helps sustain intrinsic OER activity at high current density. At the dual-phase LDH/spinel interface, abundant defects and unsaturated coordination sites are present, and the work-function difference between the phases induces directed interfacial electron transfer and redistribution. These features stabilize active centers and preserve favorable intermediate binding during prolonged electrolysis. The high-entropy effect also contributes entropy stabilization and slow ion-migration kinetics; together with intimate interphase contact, it restrains metal-ion leaching and phase evolution, maintaining structural integrity and corrosion resistance. In addition, the 3D nanosheet architecture and suitable pore channels aid electrolyte permeation, intermediate diffusion, and gas bubble disengagement, alleviating severe mass-transport constraints at 1 A cm^{-2}. Overall, these mechanisms allow the electrode to retain structural and electrochemical stability beyond 100 h, as reflected in the small voltage rise. This further supports the catalyst's potential to advance from three-electrode activity screening to industrial-level operation.

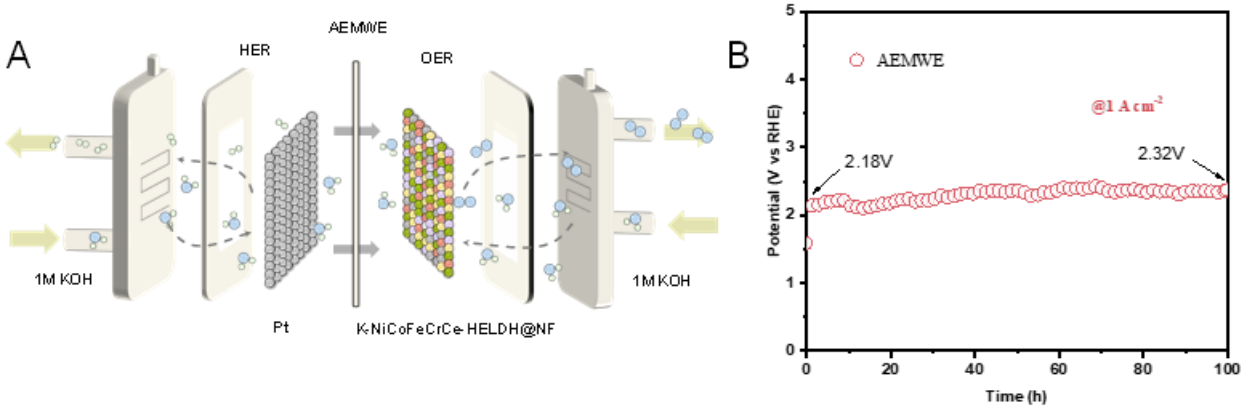


Figure 5. *(A) Schematic illustration of the AEM electrolyzer configuration of (K)-NiCoFeCrCe-HELDH/HESO@NF. (B) Long-term durability measurement was carried out for the AWE at 1 A cm^{-2}.*

The outstanding OER performance of (K)-NiCoFeCrCe-HELDH/HESO@NF originates from several coupled mechanisms rather than a single structural feature. Potassium plays a central electronic role: its low electronegativity and large ionic radius allow it to enter the HELDH lattice, where it induces lattice expansion and distortion. This perturbation alters the electronic density of states of neighboring Ni, Co, and Fe and shifts the d-band center, thereby bringing the adsorption free energies of OH*, O*, and OOH* closer to optimal and enhancing intrinsic OER activity. The dual-phase LDH/spinel heterointerface provides another level of regulation. It contains abundant defects and unsaturated coordination sites that can serve as additional catalytically active centers. Moreover, the work-function mismatch between the two phases drives directional electron transfer and redistribution across the interface, which further optimizes intermediate binding and lowers the energy barrier of the rate-determining step. Entropy stabilization also contributes. The high-entropy composition, together with sluggish ion-migration kinetics and the intimate contact between the two phases, helps suppress leaching of active metal ions and phase transformation during electrocatalysis. This preserves structural integrity and corrosion resistance over prolonged operation. Morphology matters as well. The three-dimensional nanosheet architecture and suitable pore channels improve electrolyte transport and intermediate adsorption/desorption, supporting fast reaction kinetics at high current densities. Collectively, these effects give the electrode both high activity and high stability in alkaline media. This design is also consistent with recent reports on alkali-metal (Na)-doped high-entropy hydroxides, in which oxygen nonbonding states are engineered to promote water oxidation.

4. Conclusions

A one-step hydrothermal route was used to co-deposit six metal salts—K, Ni, Co, Fe, Cr, and Ce—onto nickel foam, yielding a self-supported dual-phase high-entropy layered double hydroxide/spinel (HELDH/HESO) heterostructured electrode, (K)-NiCoFeCrCe-HELDH/HESO@NF, in which alkali metal potassium acts as a synergistic driver. The electrode features a three-dimensional nanosheet architecture and a uniform distribution of multiple elements. In 1 M KOH, it delivers current densities of 100 and 1000 mA cm^{-2} at overpotentials of only 279 and 355 mV, respectively, outperforming the K-free control. When tested in an anion exchange membrane electrolyzer under simulated industrial conditions, the cell showed a voltage increase of just about 6.4% after 100 h of continuous operation, indicating excellent long-term stability. The combined effects of K-mediated electronic regulation, dual-phase heterointerface synergy, and high-entropy stabilization enable simultaneous optimization of catalytic activity and structural durability. The preparation method is straightforward, reproducible, cost-controllable, and environmentally benign, offering a practical design strategy for efficient, stable, and low-cost non-noble-metal OER catalysts for AEM water electrolysis hydrogen production.

Abbreviations

OER	Oxygen Evolution Reaction
AEM	Anion Exchange Membrane

Author Contributions

Xin Li: Writing – original draft, Writing – review & editing

Bin Dong: Funding acquisition, Supervision, Writing – original draft, Writing – review & editing

Yong-Ming Chai: Funding acquisition, Supervision, Writing – original draft, Writing – review & editing

Funding

This work is financially supported by National Natural Science Foundation of China (22479161 and 52274308)

Data Availability Statement

The data supporting the outcome of this research work has been reported in this manuscript.

Conflicts of Interest

The authors declare no conflicts of interest.

References

[1] Y. Xun, Z. Wei, M. Li, S. Zhou, Y. Ma, W. Liu, S. Chang, J. Ding, Digital light processing of Zr-doped NiFe self-supported electrodes for efficient and stable high-current-density oxygen evolution, Virtual Phys. Prototyping 21 (2026) e2607267. https://doi.org/10.1080/17452759.2025.2607267

[2] J. He, Y. Zhao, Y. Li, Q. Yuan, Y. Wu, K. Wang, K. Sun, J. Wu, J. Jiang, B. Zhang, L. Wang, M. Fan, Joule heating-driven sp^2-C domains modulation in biomass carbon for high-performance bifunctional oxygen electrocatalysis, Nano Micro Lett. 17 (2025). https://doi.org/10.1007/s40820-025-01725-0

[3] Y. Zhai, X. Ren, T. Gan, L. She, Q. Guo, N. Yang, B. Wang, Y. Yao, S. (Frank) Liu, Deciphering the synergy of multiple vacancies in high-entropy layered double hydroxides for efficient oxygen electrocatalysis, Adv. Energy Mater. 15 (2025) 2502065. https://doi.org/10.1002/aenm.202502065

[4] E. Wallnöfer-Ogris, I. Grimmer, M. Ranz, M. Höglinger, S. Kartusch, J. Rauh, M.-G. Macherhammer, B. Grabner, A. Trattner, A review on understanding and identifying degradation mechanisms in PEM water electrolysis cells: Insights for

stack application, development, and research, Int J Hydrogen Energy 65 (2024) 381–397. https://doi.org/10.1016/j.ijhydene.2024.04.017

[5] Q. Hu, A. Li, Y. Sun, L. Liu, T. Liu, C. Li, H. Han, Tailor control of neodymium doping sites in γ-MnO_2 for stable oxygen evolution reaction in acidic electrolyte, Adv. Funct. Mater. (2025) 2423709. https://doi.org/10.1002/adfm.202423709

[6] C. Feng, Y. Zhou, M. Chen, L. Zou, X. Li, X. An, Q. Zhao, P. Xiaokaiti, A. Abudula, K. Yan, G. Guan, High-entropy spinel $(FeCoNiMnAl)_3O_4$ with three-dimensional microflower structure for stable seawater oxidation, Appl. Catal. B Environ. Energy 349 (2024) 123875. https://doi.org/10.1016/j.apcatb.2024.123875

[7] Y. Song, J. Qian, S. Li, Z. Zhao, H. Chen, K. Zou, Z. Han, Z. Li, H. Li, H. Zhou, M. Shao, Stabilizing lattice oxygen to enable durable MnO_2 electrocatalyst for simultaneous acidic hydrogen production and biomass valorization, Angew. Chem. Int. Ed. 64 (2025). https://doi.org/10.1002/anie.202502847

[8] Z. Ji, J. Sun, Y. Jin, H. Guo, H. Cheng, X. Lang, L. Chen, Y. Zhu, Q. Jiang, Charge self-modulation of the NiCo-OH/FeOOH heterostructure for industrial-current-density oxygen evolution reaction, Chemical Engineering Journal 538 (2026) 176823. https://doi.org/10.1016/j.cej.2026.176823

[9] J. Sun, N. Zhao, J. Xin, M. Yu, C. Lv, Y. Jiao, X. Wang, Orbital hybridization and adsorption modulating in Mo/P Co-doped Ni_3S_2 enables superior urea-assisted water electrolysis at industrial current density, Appl Catal, B 386 (2026) 126446. https://doi.org/10.1016/j.apcatb.2026.126446

[10] G. Shi, J. Li, T. Lu, C. Yang, Q. Xu, H. Gu, H. Tong, S. Zhao, C. Zhu, Y. Shen, J. Wu, X. Lao, P.-C. Chen, J. Li, S. Zhang, J. Shi, K.H.L. Zhang, Y.-F. Li, Z.-P. Liu, L. Zhang, Lattice O–O ligands in Fe-incorporated hydroxides enhance water oxidation electrocatalysis, Nat. Chem. 17 (2025) 1607–1614. https://doi.org/10.1038/s41557-025-01898-6

[11] J. Baek, K.S. Hamkins, Y. Li, A.T. Garcia-Esparza, T. Liu, C.-T. Kuo, J.-S. Lee, A.W. Potter, S. Kim, Y. Wang, H. Ding, J. Li, Z. Zhuo, J. Guo, M. Bajdich, X. Zheng, Modulating coordinate site occupancy in high-entropy spinel electrocatalysts, Nat Commun 17 (2026) 3540. https://doi.org/10.1038/s41467-026-70982-3

[12] F. Lu, G. Feng, H. Qi, Q. Li, L. Su, Z. Kang, Y. Hou, Z. Huang, D. Xia, Structurally ordered high-entropy intermetallics for electrocatalysis, Adv. Energy Mater. 15 (2025) e03306. https://doi.org/10.1002/aenm.202503306

[13] M. Coduri, L.R. Magnaghi, M. Fracchia, R. Biesuz, U. Anselmi-Tamburini, Assessing phase stability in high-entropy materials by design of experiments: The case of the (Mg, Ni, Co, Cu, Zn)O system, Chem. Mater. 36 (2024) 720–729. https://doi.org/10.1021/acs.chemmater.3c02120

[14] Z. Wang, S. Chen, R. Chen, H. Jiang, Y. Jiang, Q. Wei, W. Wu, J. Zhong, N. Cheng, Charge competition enhancing Ru-based high entropy oxide nanosheet for efficient and stable oxygen evolution, Applied Catalysis B: Environment and Energy 383 (2026) 126034. https://doi.org/10.1016/j.apcatb.2025.126034

[15] Q. Lu, J. Liu, X. Zou, B. Huang, W. Wu, J. Yin, Z. Liu, Y. Wang, Breaking the activity-stability trade-off of RuO_2 via metallic Ru bilateral regulation for acidic oxygen evolution reaction, Angew. Chem. Int. Ed. 64 (2025) e202503733. https://doi.org/10.1002/anie.202503733

[16] Y. Gao, M. Yan, H. Zhong, M. Li, J. Yao, B. Zhang, Compressed Co–O bonds resist chlorine corrosion to enhance the stability of chlorine-involved anodic reactions, Angew. Chem. Int. Ed. 65 (2026) e19520. https://doi.org/10.1002/anie.202519520.

[17] N. Sun, Z. Zheng, L. Jiang, G. Liu, Y. Qin, W.-H. Huang, C.-W. Pao, Z. Hu, M. Lei, T. Ying, R. Yu, K. Huang, Entropy-stabilized cation–anion vacancies coupling in high-entropy two-dimensional crystals for efficient oxygen evolution, Adv. Funct. Mater. 36 (2026) e75186. https://doi.org/10.1002/adfm.75186

[18] L. Tang, T. Zhang, Z. Cao, L. Li, X. Li, F. Wang, H. Cong, Oxophilic regulation drives the mechanism transition of NiOOH toward the oxide pathway for water oxidation, Adv Funct Materials (2026) e77785. https://doi.org/10.1002/adfm.77785

[19] W. Guan, C. Zhang, Y. Zhang, Y. Feng, Y. Mei, Q. Qi, Y. Song, J. Hu, High-entropy heterostructures modulated by oxyphilic transition metals for efficient oxygen evolution reaction, Nano Energy 134 (2025) 110528. https://doi.org/10.1016/j.nanoen.2024.110528

[20] Z. Li, Y. Jin, Z. Ji, H. Kang, X. Lang, L. Chen, Y. Zhu, Local electronic environment regulation of crystalline/amorphous NiSe/$NiFe(OH)_x$ heterostructure enhancing catalytic activity of alkaline oxygen evolution reaction, Small 22 (2026) e14445. https://doi.org/10.1002/smll.202514445

[21] H. Yang, F. Chen, X. Wang, J. Qian, J. Wang, J. Li, C. Lv, L. Li, S. Bandaru, J. Gao, Self-reconstructed spinel with enhanced SO_4^{2-} adsorption and highly exposed Co^{3+} from heterostructure boosts activity and stability at high current density for overall water splitting, Adv. Funct. Mater. 35 (2025) 2419978. https://doi.org/10.1002/adfm.202419978

[22] Z. Liu, F. Ren, M. Li, R. He, Activating inert bismuth atoms via interfacial p–d orbital hybridization: A robust strategy for efficient oxygen evolution reaction, J. Colloid Interface Sci. 727 (2027) 141556. https://doi.org/10.1016/j.jcis.2026.141556

[23] J. Li, L. Liu, D. Guan, H. Liang, Z. Lu, H. Wang, Y. Zhang, J. Tang, S. Chen, G. Feng, L. Zeng, R.V. Kumar, J. Xu, S. Ding, Y.-L. He, K. Xi, d-p Orbital Hybridization Tailoring for Boosted Redox Kinetics in Li-CO_2 Batteries, Advanced Functional Materials 36 (2026) e14223. https://doi.org/10.1002/adfm.202514223

[24] F. Wang, L. Feng, M. Zhang, H. Cong, Engineering oxygen nonbonding states in high entropy hydroxides for scalable water oxidation, Nat. Commun. 16 (2025) 6624. https://doi.org/10.1038/s41467-025-61766-2

[25] R. Zhang, X. Ji, Y. Fan, F. Yang, S. Lin, X. Lu, Local coordination engineering of NiFe-LDH catalyst with carboxylate and sodium for durable seawater oxygen evolutionNiFe-LDH, Applied Catalysis B: Environment and Energy 381 (2026) 125850. https://doi.org/10.1016/j.apcatb.2025.125850